3. American Cancer Society. *Cancer facts and figures*. Atlanta: American Cancer Society; 1991.
4. Kalse MH, Barkin J, MacIntyre JM. Pancreatic cancer: assessment of prognosis by clinical presentation. *Cancer* 1985;56:397–402.
5. Kelly DM, Benjamin IS. Pancreatic carcinoma. *Ann Oncol* 1995;6:19–28.
6. Van Dyke JA, Stanley RJ, Berland LL. Pancreatic imaging. *Ann Intern Med* 1985;102:212–217.
7. Balthazar EJ, Chako AC. Computed tomography of pancreatic masses. *Am J Gastroenterol* 1990;85:343–349.
8. Freeny PC, Marks WM, Ryan JA, Traverso LW. Pancreatic ductal adenocarcinoma: diagnosis and staging with dynamic CT. *Radiology* 1988;166:125–33.
9. Steiner E, Stark DD, Hahn PF, et al. Imaging of pancreatic neoplasms: comparison of MR and CT. *Am J Roentgenol* 1989;152:487–491.
10. Sreedharan SP, Robichon A, Peterson KE, Goetzl EJ. Cloning and expression of the human vasoactive intestinal peptide receptor. *Proc Natl Acad Sci USA* 1991;88:4986–4990.
11. Battari A, Martin J, Luis J, et al. Solubilization of the vasoactive intestinal peptide receptor from human colonic adenocarcinoma cells. *J Biol Chem* 1988;263:17685–17689.
12. Reubi JC. In vitro identification of vasoactive intestinal peptide receptors on human tumors: implications for tumor imaging. *J Nucl Med* 1995;36:1846–1853.
13. Virgolini I, Raderer M, Angelberger P, et al. Vasoactive intestinal peptide (VIP) receptor imaging for the localization of intestinal adenocarcinomas and carcinoid tumors. *N Engl J Med* 1994;331:1116–1121.
14. Virgolini I, Kurtaran A, Raderer M, et al. Vasoactive intestinal peptide receptor scintigraphy. *J Nucl Med* 1995;36:1732–1739.
15. Raderer M, Becherer A, Kurtaran A, et al. Comparison of ^{123}I-vasoactive intestinal peptide receptor scintigraphy and ^{111}In-CYT-103 immunoscintigraphy. *J Nucl Med* 1996;37:1480–1487.
16. Haegerstrand A, Jonzon B, Daalsgard CJ, et al. Vasoactive intestinal polypeptide stimulates cell proliferation and adenylate cyclase activity of cultured human keratinocytes. *Proc Natl Acad Sci USA* 1989;86:5993–5996.
17. Svoboda M, Neef de P, Tastenoy, et al. Molecular characteristics and evidence for internalization of vasoactive intestinal peptide (VIP) receptors in the tumoral rat pancreatic acinar cell line AR 4–2J. *Eur J Biochem* 1988;176:707–713.
18. Scatchard G. The attraction of proteins for small molecules and ions. *Ann NY Acad Sci* 1949;51:660–672.
19. Silverman DT, Dunn JA, Hoover RN, et al. Cigarette smoking and pancreas cancer: a case-control study based on direct interviews. *J Natl Cancer Inst* 1994;86:1510–1516.
20. Virgolini I, Yang Q, Li S, et al. Cross-competition between vasoactive intestinal peptide and somatostatin for binding to tumor cell membrane receptors. *Cancer Res* 1994;54:690–700.
21. Krenning EP, Kwekkeboom DJ, Bakker WH, et al. Somatostatin receptor scintigraphy with ^{111}In-DTPA-D-Phe1- and ^{123}I-Tyr-octreotide: the Rotterdam experience with more than 1000 patients. *Eur J Nucl Med* 1993;20:716–731.
22. Reubi JC. Neuropeptide receptors in health and disease: the molecular basis for in vivo imaging. *J Nucl Med* 1995;36:1825–1835.
23. Kato T, Fukatsu H, Ito K, et al. Fluorodeoxyglucose positron emission tomography in pancreatic cancer: an unsolved problem. *Eur J Nucl Med* 1995;22:32–39.
24. Inokuma T, Tamaki N, Torizuka T, et al. Value of fluorine-18-fluorodeoxyglucose and thallium-201 in the detection of pancreatic cancer. *J Nucl Med* 1995;36:229–235.

Location of a VIPoma by Iodine-123-Vasoactive Intestinal Peptide Scintigraphy

Irene Virgolini, Amir Kurtaran, Maria Leimer, Klaus Kaserer, Markus Peck-Radosavljevic, Peter Angelberger, Peter Hübsch, Milos Dvorak, Peter Valent and Bruno Niederle

Departments of Nuclear Medicine, Internal Medicine, Clinical Pathology, Gastroenterology, General Surgery and Radiology, University of Vienna, Vienna; Department of Radiochemistry, Research Center, Seibersdorf, Austria; and Department of Internal Medicine, Charles University of Prag, Czech Republic

A major problem in patients with small endocrine tumors is the difficulty in localizing the primary tumor site. Many endocrine tumors possess larger amounts of high affinity vasoactive intestinal peptide (VIP) binding sites compared with normal tissue or blood cells. We used radiolabeled VIP to localize the tumor site in a patient with Verner-Morrison syndrome (VMS). Under octreotide therapy, the VIP levels had declined in this patient, but a tumor site could not be detected by conventional techniques or by radiolabeled octreotide. However, using ^{123}I-VIP, the tumor was detectable in the pancreatic tail. Surgical resection of the tumor was followed by complete remission of the VMS. Expression of VIP binding sites in the tumor was confirmed by a radioreceptor assay and showed cross-competition between VIP and octreotide. The identity of the VIP binding site in the tumor was analyzed by Northern blotting and revealed the expression of somatostatin receptor subtype 3, which binds both somatostatin-14 and VIP with higher affinity than octreotide. Iodine-123-VIP scintigraphy would be an effective tracer to identity the tumor site in VMS patients.

Key Words: vasoactive intestinal peptide; Verner-Morrison syndrome; somatostatin; VIPoma; scintigraphy

J Nucl Med 1998; 39:1575–1579

In 1958, Verner and Morrison described a syndrome of watery diarrhea and hypokalemia in a patient with an islet cell tumor (*1*). The substance responsible for this syndrome was identified in 1970 (*2*) and named vasoactive intestinal peptide (VIP).

Received Aug. 5, 1997; accepted Dec. 24, 1997.

For correspondence or reprints contact: Irene Virgolini, MD, Department of Nuclear Medicine, University of Vienna, Währinger Gürtel 18-20, A-1090 Vienna, Austria.

At presentation, VIP-secreting tumors (VIPomas) can be large and hypervascular (*3*). In approximately 20% of the well-documented cases, however, these tumors are small and cannot be localized by conventional techniques (*3*). These patients represent a serious challenge for clinicians since surgery is the only form of curative treatment.

Recently, somatostatin receptor (SSTR) scintigraphy using radiolabeled octreotide has detected small neuroendocrine tumors and has been used to detect VIPomas (*4,5*).

Based on the high level expression of VIP receptors on various tumor cells, we have demonstrated that ^{123}I-VIP scintigraphy provided excellent visualization of small gastrointestinal (GI) tumors expressing receptors for VIP (*6,7*). We describe here a patient with Verner-Morrison syndrome (VMS) in whom the VIPoma could not be localized by radiolabeled octreotide, but it was identified in the pancreatic tail before surgical resection by VIP scintigraphy using ^{123}I-labeled VIP.

CASE REPORT

In November 1994, a 38-yr-old man was referred because of a 4-yr history of therapy-refractory watery diarrhea, hypokalemia and dehydration. Since 1990, the patient had been having episodes of headache, diarrhea, hypotension and tachycardia associated with progressive malabsorption. In 1992 and 1993, he was hospitalized for hypokalemia (K+ = 1.6 mmol/liter) and acute renal failure. In January 1994, an elevated serum VIP level was measured (159 pmol/liter; normal value < 8 pmol/liter), and the diagnosis of VMS was established. Normal serum values for parathyroid hormone, insulin, C-peptide, gastrin and

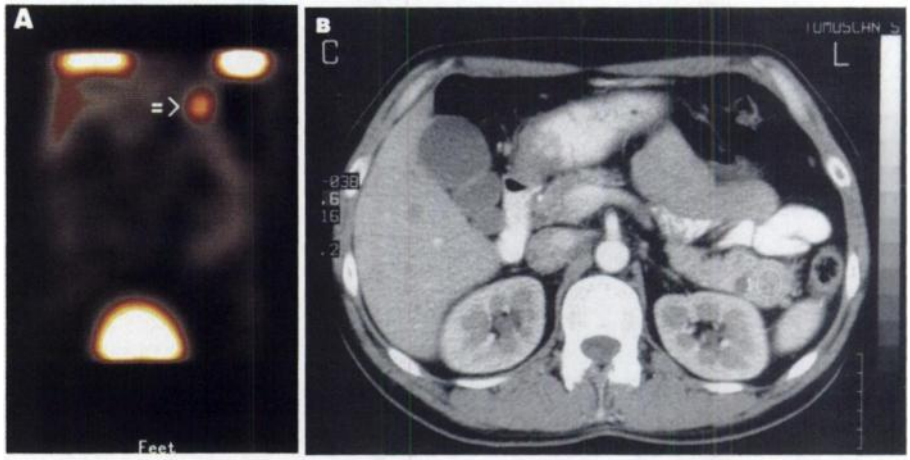

FIGURE 1. (A) Imaging of VIPoma by means of ^{123}I-VIP. Reconstruction of data obtained by SPECT 3 hr after intravenous injection of 150 MBq ^{123}I-VIP (300 pmol) depicts focal accumulation of tracer in pancreatic tail (coronal reconstruction, arrow). (B) Corresponding CT. In light of positive VIP scintigraphy, enlargement of pancreatic tail combined with loss of lobulation was interpreted as indirect sign of tumorous infiltration. Putative tumor site is marked with region of interest circle. Small pancreatic cyst is indicated by 1.

prolactin, as well as serum calcium, were obtained. In June 1994, treatment with octreotide was started (maximal dose 0.1 mg/day), and this resulted in an improvement of the VMS and stable K+ values (3.4–3.7 mmol/liter).

The patient was examined repeatedly for the presence of a tumor. In 1994, ultrasound, contrast enhanced CT, a radiograph of the small bowel (enteroclysis), upper GI endoscopy, angiography (coeliac trunk) and conventional scintigraphy of the liver and spleen were performed in addition to SSTR scintigraphy using ^{111}In-pentetic acid (DTPA)-D-Phe-1-octreotide (*6*). No tumor site was localized.

In November 1994, VIP scintigraphy using ^{123}I-labeled VIP and SSTR scintigraphy using ^{123}I-Tyr-3-octreotide were performed (after discontinuation of octreotide therapy). Iodine-123-Tyr-3-octreotide scintigraphy failed to localize the tumor, but ^{123}I-VIP scintigraphy revealed a small focus in the pancreatic tail. Based on the positive VIP scintigraphy, the tumor site was confirmed by contrast enhanced CT (spiral technique) as well as by endosonography. The tumor was resected in December 1994. Histological examination confirmed the diagnosis of a VIPoma. After surgical resection, the patient rapidly improved and treatment with octreotide was stopped. VIP serum levels normalized within 2 days after surgery (54 pmol/liter, on the day of surgery; 5 pmol/liter, 2 days later). Also, the K+ values were in the normal range after surgery.

Postoperative VIP receptor scintigraphy was negative. At 2 yr after resection of the VIPoma, the patient was still in complete remission and had gained 14 kg. He was in good health with a normal VIP serum level.

Scintigraphic Techniques and Imaging Results

VIP scintigraphy was performed as described previously (*6,7*) using high-performance liquid chromatography-purified ^{123}I-VIP administered as a single intravenous bolus injection [200 MBq; 300 pmol (1 ug)]. Planar sequential anterior-posterior images of the abdomen were recorded over 30 min (matrix 128 × 128) with a large-field-of-view Toshiba gamma camera equipped with a low-energy, general-purpose collimator. As reported previously (*7*), the lungs are the primary organ of VIP-uptake and, subsequently, the radioactivity (free ^{123}I) was excreted from the urinary tract. During the initial imaging period, a small focus of increased activity could be visualized in the left lateral part of the epigastrium. SPECT was performed with a Picker 1000 Prism gamma camera that located the tumor in the pancreatic tail (Fig. 1A).

SSTR scintigraphy was performed as described using ^{111}In-DTPA-D-Phe-1-octreotide (*5*) as well as ^{123}I-labeled Tyr-3-octreotide (*4,5*). Multiple planar and SPECT studies were performed up to 48 hr postinjection (*5*).

CT of the pancreas was performed with a Tomoscan SR7000 (Phillips, Eindhoven, The Netherlands). The first CT examination used 10-mm slices without contrast enhancement. In the second and subsequent examination, the spiral CT technique with intravenous contrast medium injection (100-ml Omnipaque 300, flow 1.5 ml/sec, delay 40 sec; slice thickness 5 mm; table speed 5 mm/sec; reconstruction index 3 mm) was used. In the third examination, a multiplanar reconstruction mode was used. In this technique, an area approximately 3 cm in diameter was detected in the pancreas in the same location as the positive VIP scintigraphy (Fig. 1B)

Surgery and Histological Examination

A left pancreatic resection with splenectomy and a radical lymphadenectomy were performed. Macroscopically, the tumor was well-encapsulated. Unexpectedly, two more lesions (less than 1 cm in diameter) were found in close proximity to the 3.5-cm (largest) in diameter nodule (1 and 2.5 cm apart from the 3.5-cm nodule). Histological examination of the 3.5-cm nodule revealed an epithelial tumor with tumor cells growing predominantly in ribbons and festoons separated by a delicate fibrovascular stroma resulting in a gyriform pattern. Tubular structures were seen occasionally. Of the two smaller nodules, one was solid and composed of clear cells, whereas the other one was characterized by extensive fibrosis. Immunohistochemistry was performed on the paraffin-embedded sections. Indirect immunoperoxidase staining technique was used.

Most of the tumor cells expressed VIP (Fig. 2; rabbit polyclonal antibody against VIP, Biogenix, San Ramon, CA; dilution 1:20 goat serum) and glucagon (rabbit polyclonal

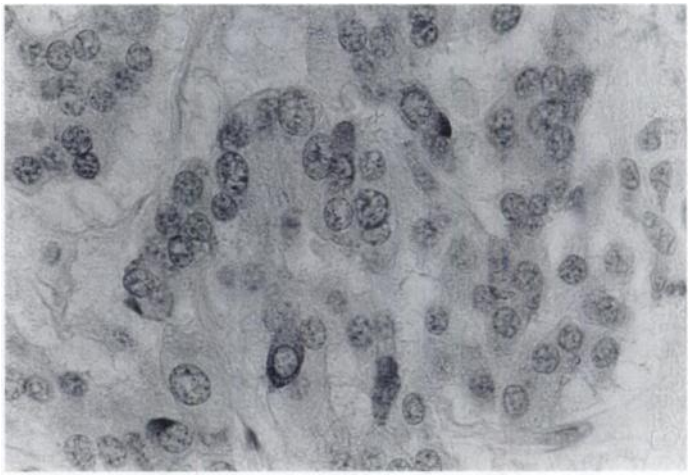

FIGURE 2. Immunohistochemical detection of VIP in VIPoma tissue using indirect immunoperoxidase technique.

TABLE 1
Binding of Labeled VIP and Octreotide Analogs to VIPoma

			IC_{50} values (nM)				
	Sites/cell	K_d (nM)	SST-14	VIP	OCT	^{123}I-Tyr-3-OCT	^{111}In-DTPA-D-Phe-1-OCT
^{123}I-VIP	1.9×10^{14}	0.8	3.5	0.9	2.0	2.1	3.5
	[2.5×10^{11}	2.5	9.8	2.5	10.3	12.3	14.4]
^{123}I-Tyr-3-OCT	2.2×10^{14}	2.0	6.2	1.5	2.3	2.1	2.9
	[2.3×19^{11}	3.5	6.3	8.5	np	np	np]
^{111}In-DTPA-D-Phe-1-OCT	1.8×10^{14}	4.7	np	3.8	2.3	2.9	4.5
	[2.5×10^{11}	4.9	8.4	12.6	np	3.2	np]

The concentration of labeled ligand used for the determination of the iC_{50} (displacement study) was identical with the K_d value obtained by the saturation study.

Values in brackets [ ] are the results for peripheral mononuclear cells.

K_d = dissociation constant; IC_{50} = concentration of unlabeled ligand causing 50% inhibition of labeled ligand binding; np = not performed.

antibody, Chemicon, Temecula, CA; dilution 1:2000 goat serum). A positive reaction with antibodies against the neuroendocrine markers neuron specific enolase, and chromogranin A was found by immunohistochemistry, whereas negative reactions were found for serotonin, gastrin, pancreatic polypeptide, insulin, somatostatin (SST) and alpha-human chorionic gonadotropin. The lymph nodes (12 nodes available in total) and spleen were free of tumor cells. Tissue specimens of the 3.5-cm VIPoma were used for the in vitro studies that we describe later.

In Vitro Receptor Evaluation

VIPoma tissue obtained at surgery was subjected to in vitro binding studies using ^{123}I-VIP, ^{123}I-Tyr-3-octreotide and ^{111}In-DTPA-D-Phe-1-octreotide as radioligands and unlabeled VIP, octreotide, Tyr-3-octreotide, DTPA-D-Phe-1-octreotide and SST-14 as competitors in in vitro displacement studies. At the same time, peripheral mononuclear cells (PMNC) from the patient were run in control studies. All binding studies were performed as described previously (*8*). The results of our study (Table 1) indicate the presence of VIP as well as octreotide binding sites in the VIPoma tissue. When compared with normal cells, a higher level of VIP/octreotide receptors was observed. In line with data obtained previously with other tumors (*6,8*), cross-competition between VIP and octreotide binding to VIPoma cells was demonstrable as indicated by IC_{50} values (concentrations causing half-maximal inhibition) in the lower nanomolar range (Table 1).

mRNA Analysis of Peptide Receptors

To detect the peptide binding site responsible for VIP binding, Northern blot analysis of mRNA obtained from the VIPoma was performed using cDNA probes. RNA of the tumor tissue was extracted using the trizol-reagent (Gibco/BBL, Vienna, Austria) according to the instructions of the manufacturer. Northern transfer of 20 μg of total RNA was performed as described previously (*9*). After transfer to Schleicher & Schuell Nytran membranes (Schleicher and Schuell, Vienna, Austria) by overnight capillary blotting, the RNA was fixed to the membrane by ultraviolet-crosslinking. After separation in an agarose-gel, probes were purified with a Qiaex gel purification kit (Qiagen, Hilden, Germany) and labeled using the Redivue random prime labeling kit (Amersham, Vienna, Austria) and ^{32}P-dCTP (Amersham). Hybridization was performed as described previously (*9*). The VIPoma expressed large amounts of SSTR subtype 3 mRNA (Fig. 3A) These cells were found to express low amounts of SSTR2, 4 and 5 and VIPR2, and they lacked SSTR1 and VIPR1. PMNCs expressed only very low amounts of SSTR3 (Fig. 3B) and SSTR4 > SSTR5 = VIPR2, and they did not express SSTR1 and 2 and VIPR1.

Analysis of the Transfected SSTR3

To further analyze whether SSTR3 would bind ^{123}I-VIP, receptor transfection studies were performed. Transient transfection of COS-7 cells (ATCC, Rockville, MD) with SSTR3-cDNA was performed using the N-[1-(2,3-dioleoyloxyl)

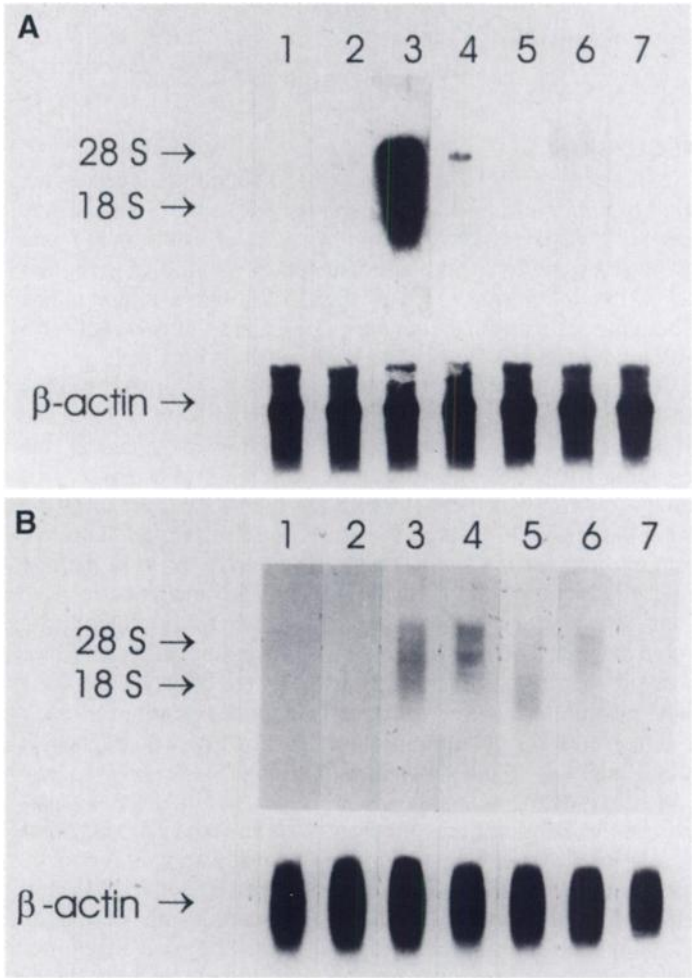

FIGURE 3. RNA analysis of VIPoma by Northern blotting. Twenty μg of total RNA (A) from VIPoma tissue or (B) PMNCs were applied to each lane. Hybridization was performed as follows (upper panel, A and B): Lane 1, hSSTR1; Lane 2, hSSTR2; Lane 3, hSSTR3; Lane 4, hSSTR4; Lane 5, hSSTR5; Lane 6, rVIP-R2; Lane 7, hHIV-8c. Lower panel (A and B): control hybridization was performed using human beta-actin probe.

TABLE 2
Binding of Labeled VIP and Octreotide Analogs to SSTR3 Subtype Receptors

			IC_{50} values (nM)		
	Sites/cell	K_d (nM)	SST-14	VIP	OCT
^{125}I-SST-14	$3.4 \pm 0.4 \times 10^3$	0.4 ± 0.3	0.5 ± 0.3	1.2 ± 0.5	17 ± 5
^{123}I-VIP	$3.8 \pm 0.4 \times 10^3$	1.5 ± 0.6	4.2 ± 1.9	1.5 ± 0.8	12 ± 6
^{123}I-Tyr-3-OCT	$1.2 \pm 0.7 \times 10^3$	32 ± 8	34 ± 12	18 ± 13	27 ± 11
^{111}In-DTPA-D-Phe-1-OCT	$1.1 \pm 0.5 \times 10^3$	31 ± 9	42 ± 17	21 ± 12	35 ± 14

Values are means ± s.d. of six independent experiments. The concentration of labeled ligand used for the determination of the IC_{50} (displacement study) was identical with the K_d value obtained by the saturation study.
K_d = dissociation constant; IC_{50} = concentration of unlabeled ligand causing 50% inhibition of labeled binding.

probyl]-N,N,N,-trimethylammoniummethyl sulfate transfection agent (DOTAP) transfection reagent (Boehringer Mannheim, Mannheim, Germany). Intact transfected COS-7 cells (5×10^5 cells per tube) were subjected to binding studies as described (*8*) using labeled and unlabeled ligands. Table 2 shows that the binding of ^{125}I-Tyr-11-SST-14 (Amersham, Buckinghamshire, UK) to SSTR3 was displaced by unlabeled SST-14 and VIP and less effectively also by unlabeled octreotide. Vice versa, the binding of ^{123}I-VIP to SSTR3 was displaced by SST-14, but also by octreotide, however, with lower potency. Iodine-123-Tyr-3-octreotide and ^{111}In-DTPA-D-Phe-1-octreotide bound to SSTR3 with lower affinity when compared with the binding of ^{123}I-VIP and ^{125}I-Tyr-11-SST-14 to SSTR3; however, competition by unlabeled VIP for ^{123}I-Tyr-3-octreotide and ^{111}In-DTPA-D-Phe-1-octreotide binding to SSTR3 was observed as well.

DISCUSSION

In patients with VMS, it may be difficult to localize the primary tumor site by conventional techniques (*3*). This article presents a patient with VMS with negative results in CT and SSTR scintigraphy using radiolabeled octreotide (*5*). Iodine-123-VIP scintigraphy (*6*) was able to localize a tumor in the pancreatic tail; surgical resection confirmed the presence of a VIPoma and led to a complete remission of the VMS.

VIPomas usually are slow-growing, albeit malignant, tumors (*3*). Such tumors may not be detectable in an early stage of the disease. It also may take time until clinicians consider the possibility of VMS, as in this case. Although the majority of patients with VMS (68%) may have metastatic spread at the time of surgery (*10*), surgery is the most effective and curative form of therapy for VIPomas (*10*). Alternative forms of therapy are chemotherapy and treatment with the SST analog octreotide. Such alternative treatments are used when the tumor site remains undetectable or in cases of incurable disease. Since most (80%) of the VIP-producing adenomas are located in the distal portion of the pancreas, partial pancreatectomy also may be considered for patients in whom severe VMS is diagnosed, but no tumor is found preoperatively (*3*).

In this patient, typical VMS with elevated VIP levels was diagnosed. Although the diagnosis was established long after the onset of symptoms, no primary tumor site was found by conventional techniques including contrast enhanced CT and selective angiography. Following treatment with octreotide (*11*), the clinical situation improved and the VIP levels declined. However, because of the considerable risk of tumor growth and metastases formation, as well as the uncertain long-term consequences of octreotide therapy, there were further attempts to detect the tumor using radiolabeled octreotide and, subsequently, VIP scintigraphy. The use of radiolabeled VIP was based on the expression of VIP-receptors on the VIPoma cell tissue (*8*). The VIP levels had declined to near normal so that it was expected that radiolabeled VIP would be able to bind to unoccupied VIP receptors in vivo. Indeed, the in vivo uptake of ^{123}I-VIP by lung tissue in this patient was indistinguishable from other tumor patients (*5*), and the tumor was detectable by scintigraphy (Fig. 1A). Binding of ^{123}I-VIP to the resected VIPoma tissue also could be demonstrated by radioreceptor analysis (Table 1).

The reason for the divergent scintigraphic results (VIP-positive, SRIF/octreotide-negative) remains unknown at present. One explanation could be a difference in the distribution of the two tracers in the tissues. Indeed, our previous data suggested that ^{123}I-VIP is more effective than ^{111}In-DTPA-D-Phe-1-octreotide in localizing tumor sites in the GI tract (*6*). This may be due to the relatively low abdominal background activity obtained after injection of ^{123}I-VIP as opposed to the high normal abdominal background activity obtained after injection of ^{123}I-Tyr-3-octreotide and ^{111}In-DTPA-D-Phe-1-octreotide Thus, the detection limit (size of the tumor) for GI tumors for ^{123}I-VIP scintigraphy may be lower when compared with the SSTR scintigraphy. Another possible explanation for the different scintigraphic results could be that the target peptide receptors bound VIP more effectively in vivo than octreotide. However, this possibility seems unlikely since in our in vitro binding studies the VIPoma bound both VIP and octreotide with almost equally high affinity (Table 1) and with K_d values in the low nanomolar range.

Recent data suggest that several peptide receptors including SRIF are involved in VIP binding to tumor cell membranes (*8*). The identity of the receptor-subtype involved in VIP binding of tumor cells in this patient remains unknown. Northern blot experiments using cDNA probes (Fig. 3) revealed strong expression of the SRIF subtype 3 in tumor cells, but not in PMNCs. Another receptor potentially involved in VIP binding, i.e., VIPR2, was also detected, however, the amount of expressed mRNA was rather low when compared with SSTR3. In subsequent experiments with transfected COS-7 cells expressing SSTR3 (Table 2), specific binding of ^{125}I-Tyr-11-SST-14, ^{123}I-VIP, ^{123}I-Tyr-3-octreotide as well as ^{111}In-DTPA-D-Phe-1-octreotide was demonstrable, however, with different binding affinities. In particular, ^{123}I-VIP bound with similar affinity to ^{125}I-SST-14 to SSTR3, whereas radiolabeled octreotide had lower affinity for SSTR3. The binding of ^{125}I-Tyr-11-SST-14 to SSTR3 was more effectively displaced by unlabeled VIP as compared with octreotide. Despite the fact of lower binding affinities for the radioligands, cross-competition between these ligands for SSTR3 binding was demonstrable in a reasonable affinity range of < 50 nmol/liter (Table 2). Since the VIPoma in this study also showed binding of both ligands and a cross-competition, possibly the SSTR3 was the in vivo target site of

^{123}I-VIP binding. Whether this may be the case in all VIPomas, and whether all VIPomas can be detected by VIP scintigraphy remains unclear.

CONCLUSION

A small VIPoma was detected by ^{123}I-VIP scintigraphy before its successful surgical removal. We recommend VIP scintigraphy in VMS patients with tumor sites that are undetectable by conventional imaging before surgical intervention.

ACKNOWLEDGMENTS

The plasmids containing the receptor cDNAs for the human SSTRs 1 through 4 (pCMV-hSSTR 1, 3–4; phSSTR2) were provided by Dr. G. Bell (Howard Hughes Institute, Chicago, IL). The plasmid carrying the hSSTR5 was donated by Dr. A.M. O'Carroll (National Institutes of Health, Bethesda, MD). The clone phVIPR2 was provided by Dr. M. Svoboda (Universite Libre de Bruxelles, Brussels, Belgium) and the clone phIVR-8c (VIPR1) by Dr. A. Couvineau (Institute National de la Sante et de la Recherche Medicale, Paris, France).

REFERENCES

1. Verner JV, Morrison AB. Islet cell tumor and a syndrome of refractory watery diarrhea and hypokalemia. *Am J Med* 1958;25:374–380.
2. Said SI, Mutt V. Polypeptide with broad biological activity. Isolation from small intestine. *Science* 1970;169:1217–1218.
3. Mekhjian HS, O'Dorisio TM. VIPoma syndrome. *Semin Oncol* 1987;14:282–291.
4. Lamberts SWJ, Bakker WH, Reubi JC, Krenning EP. Somatostatin receptor imaging in the localization of endocrine tumors. *N Engl J Med* 1990;323:1246–1249.
5. Krenning EP, Kwekkeboom DJ, Pauwels S, Kvols K, Reubi R. Somatostatin receptor scintigraphy. *Nuclear Med Ann* 1995;20:716–731.
6. Virgolini I, Raderer M, Kurtaran A, et al. Iodine-123-vasoactive intestinal peptide for the localization diagnosis of intestinal adenocarcinomas and endocrine tumors. *N Engl J Med* 1994;331:1116–1121.
7. Virgolini I, Kurtaran A, Raderer M, et al. Vasoactive intestinal peptide receptor scintigraphy. *J Nucl Med* 1995;36:1732–1739.
8. Virgolini I, Yang Q, Li SR, et al. Cross-competition between vasoactive intestinal peptide (VIP) and somatostatin for binding to tumor cell receptors. *Cancer Res* 1994;54:690–700.
9. Sambrook J, Fritsch EF, Maniatis T, eds. *Molecular cloning*, 2nd ed. Cold Spring Harbor, NY: Cold Spring Harbor Laboratory Press; 1989:740.
10. McLeod MK, Few JW, Shapiro B. Diagnostic advances in APUDomas and other endocrine tumors: imaging and localization. *Semin Oncol* 1993;9:399–432.
11. Lamberts SWJ, Lely AJ, Herder WW, Hofland LJ. Octreotide. *N Engl J Med* 1996;334:246–254.

Indium-111-DTPA-Folate as a Potential Folate-Receptor-Targeted Radiopharmaceutical

Carla J. Mathias, Susan Wang, David J. Waters, John J. Turek, Philip S. Low and Mark A. Green

Departments of Medicinal Chemistry and Molecular Pharmacology, Chemistry, Veterinary Clinical Sciences and Veterinary Physiology and Pharmacology, Purdue University, West Lafayette, Indiana

Indium-111-labeled diethylenetriamine pentaacetic acid (DTPA)-folate was evaluated as a radiopharmaceutical for targeting tumor-associated folate receptors. **Methods:** Athymic mice were subcutaneously inoculated with ~1.8 × 10^6 folate receptor-positive KB (human nasopharyngeal carcinoma) cells, yielding 0.2- to 0.6-g tumors in 15 days, at which time ^{111}In-DTPA-folate, ^{111}In-DTPA or ^{111}In-citrate was administered by intravenous injection. **Results:** The ^{111}In-DTPA-folate conjugate afforded marked tumor-specific ^{111}In deposition in vivo using this mouse model. The involvement of the folate receptor in mediating tumor uptake of ^{111}In-DTPA-folate was demonstrated by the blocking of tumor uptake by coadministration of free folic acid (intravenous). The ^{111}In-DTPA-folate also shows folate receptor-mediated uptake and retention in the kidneys, presumably reflecting radiotracer binding to folate receptors of the proximal tubules. In control experiments, the ^{111}In-citrate radiopharmaceutical precursor was also shown to afford significant tumor uptake of ^{111}In, but with much poorer tumor-to-background tissue contrast than that obtained with ^{111}In-DTPA-folate. Unconjugated ^{111}In-DTPA showed no tumor affinity. **Conclusion:** Indium-111-DTPA-folate appears suitable as a radiopharmaceutical for targeting tumor-associated folate receptors.

Key Words: indium-111-diethylenetriamine pentaacetic acid folate; folate receptor; tumor targeting

J Nucl Med 1998; 39:1579–1585

The tumor cell membrane-associated folate receptor is a potential molecular target for selective radiopharmaceutical delivery to ovarian, endometrial and other human tumors known to overexpress folate-binding protein (FBP). The folate receptor is known to be overexpressed by a variety of neoplastic tissues, including breast, cervical, ovarian, colorectal, renal and nasopharyngeal tumors, while being highly restricted in most normal tissues (*1–10*). Previously, it has been shown that this receptor system can be targeted in vitro and in vivo with low molecular weight folate-chelate conjugates such as ^{67}Ga-deferoxamine-folate and ^{111}In-diethylenetriamine pentaacetic acid (DTPA)-folate (*11–15*). This study was undertaken to better characterize the ability of ^{111}In-DTPA-folate to target tumor folate receptors in vivo using an athymic mouse tumor model.

Received Jul. 11, 1997; revision accepted Dec. 19, 1997.

For correspondence or reprints contact: Mark A. Green, PhD, Professor of Medicinal Chemistry, Purdue University, 1333 Pharmacy Building, West Lafayette, IN 47907-1333.

MATERIALS AND METHODS

General

A Capintec CRC12R radionuclide dose calibrator (Capintec, Inc., Ramsey, NJ) was used for assays of ^{111}In radioactivity in the μCi-mCi range, whereas low-level (<0.01 μCi) samples of ^{111}In were counted in a Packard 5500 automatic gamma scintillation counter with a 3-in. large-bore NaI(Tl) crystal. Folate-deficient rodent chow was obtained from ICN Biomedicals (Costa Mesa, CA) and UV-irradiated before use. The DTPA-folate conjugate (Fig. 1) was prepared as described previously (*15*)

Preparation of Indium-111 Radiotracers

The ^{111}In-DTPA-folate conjugate, ^{111}In-DTPA and ^{111}In-citrate were prepared from no-carrier-added ^{111}In-indium(III)-chloride (Mallinckrodt, Inc., St. Louis, MO). Briefly, to prepare ^{111}In-DTPA-folate, the dilute HCl solution of $^{111}In^{3+}$ was buffered by addition of sodium citrate, followed by addition of an aqueous solution of the DTPA-folate ligand. Labeling was always complete